2008-01-2407
SAND2008-8208C

Effects of LIF Tracers on Combustion in a DI HCCI Engine

Russell P. Fitzgerald and Richard R. Steeper
Sandia National Laboratories

Jordan A. Snyder
Stanford University

ABSTRACT

Many experimental efforts to track fuel-air-residual mixture preparation in internal combustion engines have employed laser induced fluorescence (LIF) of tracers. Acetone and 3-pentanone are often chosen as tracers because of their relatively strong LIF signal, weak quenching, and reasonable match to thermo-chemical properties of common fuels such as iso-octane. However, the addition of these tracers to fuel-air mixtures could affect combustion behavior. In this work, we assess these effects to better understand limitations of tracer-based engine measurements.

The effects of tracer seeding on combustion phasing, duration, and variation are studied in an HCCI engine using a recompression strategy to accommodate single- and multi-stage-ignition fuels. Using direct-injected (DI) fuels iso-octane and n-heptane, comparisons are made of combustion performance with and without seeding of the intake air (air seeding, as opposed to the more common fuel seeding, is a variation of LIF used to measure residual-gas concentration). Chemical and premixing effects of tracer addition are distinguished by substituting equivalent amounts of fuel for the tracer. Chemical kinetic simulations of iso-octane and n-heptane oxidation help explain the experimentally determined trends.

Results show that the phasing of iso-octane combustion can be significantly impacted by premixing effects because of the sensitivity of ignition to charge temperature. For n-heptane, the chemical effects of tracer addition are shown to be more pronounced because of impact on low-temperature heat release. Acetone retards the combustion for both single- and two-stage-ignition fuels, whereas 3-pentanone advances iso-octane combustion while retarding n-heptane. Overall, we found that the impact of tracer addition is modest for the chosen operating conditions since varying the intake temperature can easily compensate for it.

INTRODUCTION

Planar laser-induced fluorescence (PLIF) of fuel tracers is used extensively to track fuel/air mixture preparation in IC engines [1-2]. By recording the fluorescence signal from two different tracers, or fluorescence from a single tracer excited by two different laser wavelengths, the diagnostic is capable of measuring simultaneous composition and temperature distributions [3-4]. In recent work [5-6], Rothamer et al. have optimized a two-wavelength PLIF technique to quantify in-cylinder distributions of residual gas fraction (RGF) and temperature in our automotive HCCI engine. In this variation of the PLIF diagnostic, both fuel and air are seeded with tracer, and RGF distribution is determined as the complement of the fluorescence signal, thereby earning the name *negative PLIF* or nPLIF [7]. An important consideration when applying such LIF diagnostics in engines is the risk of tracer addition affecting combustion performance—the current study is motivated by the need to assess this risk.

While there is abundant literature describing relevant physical and photo-physical properties of commonly used LIF tracers, there have been relatively few studies to investigate the chemical effect of tracers on combustion. Practitioners typically match important thermodynamic properties of tracers with fuels they track (e.g., boiling point and heat of vaporization), thereby increasing confidence that fuel and tracer will behave similarly through the evaporation and mixing processes. But little information is available for the subsequent combustion process. Neij, et al. [8] attempted to measure the effect of 3-pentanone addition to iso-octane and n-heptane on flame speeds in a spark-ignited engine. The experiment was inconclusive beyond a statement that any changes must be less than 20%. Zhang, et al. [9] performed similar tests and concluded that the addition of 3-pentanone or toluene to iso-octane did not negatively impact combustion performance in their spark-ignited engine.

Table 1: Fuel and Tracer Properties

Fuel/tracer	Molecular Weight [g/mol]	Boiling Point [K]	Heat of Combustion [J/mg]	Stoichiometric Fuel/Air Ratio [-]
iso-octane (IO)	114.2	372	44.4	15.1
n-heptane (NH)	100.2	371	44.5	15.1
3-pentanone (3P)	86.1	375	33.4	11.2
acetone (AC)	58.1	329	28.6	9.5

PLIF tracer concentrations are typically kept low for both diagnostic (e.g., attenuation, saturation) and engine-performance reasons. Thus for our nPLIF technique we use tracer mole fractions of about 0.2 %, but because the entire air stream is seeded, the tracer can constitute up to 15% of the total chemical energy per cycle. This large tracer fraction could have a substantial chemical effect on combustion. In addition, because the tracer is premixed with air well upstream of the cylinder, substituting tracer for direct-injected fuel is likely to have a thermodynamic premixing effect as well. The primary objective of this work is to quantify effects of tracer addition on combustion performance in order to assess the relevance of applying our PLIF measurements in conventional HCCI engines.

For this study, we have selected two fuels and two tracers. The choice of iso-octane and n-heptane as fuels allows us to examine effects of tracer seeding on both single- and two-stage-ignition fuels. For tracers, we selected acetone and 3-pentanone. They are extensively used in LIF applications for several reasons: strong signal, weak quenching, and well characterized photo-physical properties [10-13]. Table 1 provides a list of thermo-chemical properties for the fuels and tracers used in this study.

EXPERIMENTAL APPROACH

Experiments were carried out in our automotive HCCI research engine [14] configured with all-metal components to extend the range and duration of the tests. Short dwell (145 CAD) cams allow negative-valve-overlap (NVO) operation, providing the elevated RGF levels required to burn high-octane fuels such as iso-octane in our facility. The pent-roof head houses two intake valves and a single exhaust valve, as well as a vertical, centrally-located, 8-hole direct injector. The head also includes two spark plug ports, but they were plugged for these HCCI experiments. Additional engine specifications are listed in Table 2.

Table 2: HCCI Engine Specifications for NVO Operation

Bore	92 mm
Stroke	95.25 mm
Geometric Compression Ratio	11.5
Intake Valve Opening	57 CAD aTDC*
Intake Valve Closing	202 CAD aTDC
Exhaust Valve Opening	202 CAD bTDC
Exhaust Valve Closing	57 CAD bTDC

*aTDC = after top dead center

Valve event timings (Table 2) were selected to accommodate operation with both iso-octane and n-heptane fuels. The selected negative overlap measures 114 CAD, producing a residual gas fraction estimated to range from 37-46% (based on parameters determined at exhaust valve closing). This RGF is appropriate since it allows fired operation for both iso-octane and n-heptane; phasing near TDC can be achieved for both by varying intake temperature from 476 K (for iso-octane) to 333 K (for n-heptane). The coolant temperature was likewise decreased for the n-heptane tests to 333K (see Table 3).

Both premixed and direct-injected fueling are used for the experiments. Premixing is accomplished using a piston pump to meter tracer (or fuel) to a heated reservoir on the inlet air line located 1 m upstream of the intake plenum. The tracer mass flow is measured using a precision scale, the air flow rate is metered using a sonic orifice, and temperature is controlled with a series of heaters on the air lines between the sonic orifices and the engine.

Combustion performance is compared using cylinder-pressure data from a piezoelectric transducer recorded every quarter crank-angle degree and averaged over 50 engine cycles. The apparent heat-release rate is calculated from filtered pressures using conservation of energy analysis and ideal-gas assumptions presented in Ref. [15]. Combustion phasing is quantified in terms of the location of 50% of the cumulative main heat release (CA50).

The goal of quantifying effects of tracer addition was approached through the following experimental plan outlined in Tables 4 and 5. The two base fuels (identified in the top row of each table) are tested with each of three different tracers (second row of the tables): 3-pentanone, acetone, and the other fuel used as a “tracer” (i.e., iso-octane or n-heptane). For each of these tracers, we conducted a series of three tests identified in the third row of Tables 4 and 5: (i) A tracer test (abbreviated *TR*) designed to duplicate conditions of a typical nPLIF experiment, that is, the tracer is premixed in the intake

Table 3: Operating Conditions for Each Base Fuel Tested

Base Fuel:	**iso-octane**	**n-heptane**
Intake air temperature	480 K	333 K
Residual Gas Fraction	40-46%	37-39%
Coolant Temperature	363 K	333 K
Intake Manifold Pressure	100 kPa	
Fuel Injection Pressure	10 MPa	
Engine Speed	1200 RPM	

Table 4: Test Matrix for iso-Octane Base Fuel

Base fuel	**iso-Octane**								
Tracer	**3-Pentanone**			**Acetone**			**n-Heptane**		
Test abbreviation; description	**TR** Premix = 3P	**PM** Premix = IO	**DI** All = DI IO	**TR** Premix = AC	**PM** Premix = IO	**DI** All = DI IO	**TR** Premix = NH	**PM** Premix = IO	**DI** All = DI IO
Premix mass [mg/cycle]	2.0	1.5	0	1.35	0.8	0	2.3	2.3	0
DI mass [mg/cycle]	9.8	9.8	11.3	9.8	9.8	10.6	9.8	9.8	12.1
Intake air [mg/cycle]	336	336	336	336	336	336	337	337	337
Tracer mol% of tot. fuel	21%	–	–	21%	–	–	21%	–	–
Tracer mol% of air	0.2%	–	–	0.2%	–	–	0.2%	–	–
Intake φ	0.52			0.49			0.55		
HOC [J/cycle]	502			474			537		

Table 5: Test Matrix for n-Heptane Base Fuel

Base fuel	**n-Heptane**								
Tracer	**3-Pentanone**			**Acetone**			**iso-Octane**		
Test abbreviation; description	**TR** Premix = 3P	**PM** Premix = NH	**DI** All = DI NH	**TR** Premix = AC	**PM** Premix = NH	**DI** All = DI NH	**TR** Premix = IO	**PM** Premix = NH	**DI** All = DI NH
Premix mass [mg/cycle]	1.7	1.2	0	1.2	0.7	0	2.3	2.3	0
DI mass [mg/cycle]	7.3	7.3	8.5	7.3	7.3	8.0	7.3	7.3	9.5
Intake air [mg/cycle]	412	412	412	406	406	406	423	423	423
Tracer mol% of tot. fuel	21%	–	–	21%	–	–	21%	–	–
Tracer mol% of air	0.15%	–	–	0.15%	–	–	0.15%	–	–
Intake φ	0.31			0.30			0.34		
HOC [J/cycle]	380			357			423		

air, and the base fuel is direct injected; (ii) A second test repeating the first, but with the tracer replaced by an equivalent amount of premixed base fuel (abbreviated *PM*); (iii) A final test with no tracer and all the fuel direct injected (abbreviated *DI*). We selected these three tests to help sort out possible chemical and thermodynamic effects of tracer addition for our nPLIF diagnostic: comparing combustion performance from the PM and DI experiments should quantify differences due to premixing a portion of the fuel, and then comparing the TR and PM results allows an assessment of tracer chemical effects.

The second column of Table 4 (i.e., the iso-octane-base-fuel/3-pentanone-tracer/TR test) represents a test conducted at typical nPLIF experiment conditions. Parameters selected for the other tests are related to these values in the following way. The amount of premixed tracer (2.0 mg/cycle of 3P), direct-injected base fuel (9.8 mg/cycle of IO), and intake air (336 mg/cycle) represents a total intake phi of 0.52. For the next test in Table 4 (PM), the amount of DI fuel and the intake air are held constant, but the premixed mass becomes an equivalent amount of IO—where *equivalent amount* is defined as the mass of fuel or tracer required to keep phi and heat-of-combustion (HOC) values approximately constant. This approach is intended to eliminate load effects on combustion performance for each series of tests. Parameters for the third (DI) test are the same as the PM test, except all fuel is direct injected, so phi and HOC again remain constant.

The same approach is applied to select parameters for the three iso-octane-base-fuel/acetone-tracer tests in Table 4. The acetone-tracer/TR test uses the same values of DI fuel and intake air as above, and the premixed mass is again adjusted to maintain approximately constant intake phi and HOC values. Selection of parameters for the next two (PM and DI) tests proceeds as in the last paragraph and selection of the remaining parameters in Table 4 follows similarly.

Imposing a constant seeding mole fraction (based on requirements of the nPLIF diagnostic) leads to differences in the load (HOC) for each test series (as shown in the bottom row of Table 4) due to differences in tracer heating values. Although moderate variations in combustion phasing and efficiency *between series* will result, this does not significantly impact overall conclusions about chemical and premixing effects of seeding made based on comparisons at constant load *within a series*.

To use the same valve timing for the n-heptane-base-fuel tests (Table 5) as for the iso-octane tests, we had to decrease intake air temperature substantially and reduce the total fuel load to avoid early combustion phasing. The cooler air meant we had to increase flow to maintain a manifold pressure of 1 bar. These factors combined to reduce values of tracer/air mole ratios, intake phi, and HOC for the n-heptane tests. Other values in Table 5 were selected using the same approach described for Table 4.

Considerable effort was required to control operating parameters for these experiments. Combustion performance during HCCI NVO operation is very sensitive to gas and surface temperatures, and achieving steady-state operation requires long run times. In addition, we observe that the fuel-delivery rate of our DI fuel injector is sensitive to operating conditions, so that duplicating target values in Tables 4 and 5 is difficult. As a result, distinguishing the effects of tracer addition from effects of varying operating conditions is challenging. Nonetheless, the paper identifies several important qualitative trends that derive from the data.

MODELING APPROACH

To confirm and explain experimental trends observed for mixtures of fuel and tracer, CHEMKIN simulations of combustion were performed using the 0-D Closed Internal Combustion Engine Simulator by Reaction Design [16] combined with chemical kinetic mechanisms distributed by Lawrence Livermore National Laboratory [17]. Separate kinetic mechanisms for iso-octane, n-heptane, and PRF blends (i.e., mixtures of iso-octane and n-heptane) [18-20] allowed simulation of single-zone reactions and corresponding pressure profiles, heat-release rates, and species time histories.

Using temperatures, intake air amounts, residual gas fractions, and fueling amounts from the experiments, initial conditions for the model were specified at bottom dead center (BDC) of compression. The initial composition of the charge was calculated using the amount of air, fuel, and tracer introduced into the chamber plus the retained residual mass and composition, which was based on products of complete combustion in excess air. BDC charge temperature is approximated by calculating the mass-averaged temperature of the retained residuals and the intake air.

The model's heat transfer correlation was adjusted to help match simulated and experimental pressure traces. In addition, for the n-heptane base-fuel simulations, intake temperatures had to be artificially increased by about 30 K to achieve combustion phasing similar to the experiments. This adjustment stems from known difficulties phasing the characteristic low-temperature heat release (LTHR) of n-heptane during HCCI combustion [21-22]. Still, by maintaining realistic conditions and a consistent approach from test to test, the model competently predicts experimentally observed trends, offering insight into the combustion behavior of iso-octane and n-heptane.

In addition to performing 0-D engine simulations, CHEMKIN was also used to simulate ignition delay times for the base fuels and tracers of interest in this study. Ignition delays for each were determined for stoichiometric conditions, constant pressure of 12 atm, and for temperatures ranging from 900 to 1400K. The same simulations were also carried out over a range of pressures in order to validate the model with available shock tube ignition time measurements for each of the constituents.

EXPERIMENTAL AND COMPUTATIONAL RESULTS

EFFECT OF FUEL PREMIXING IN THE INTAKE PLENUM

Before looking at the chemical effect of seeding the intake air with tracer, it is helpful to establish the effect of premixing a portion of the fuel in the intake air plenum (PM) rather than mixing all of it in the cylinder via direct injection (DI). Because three different tracers are tested for each fuel, three different load levels of base fuel are needed to maintain the HOC for each comparison. Indicated mean effective pressure (IMEP) and combustion phasing (CA50) of the DI and PM tests for each load level of iso-octane are shown in Figure 1 to illustrate the effect of premixing on combustion. Results for 50 consecutive cycles are plotted along with calculated mean values for each test and calculated coefficients of variation (COV) of IMEP.

At the highest iso-octane fuel load (12.1 mg), there is a clear separation of the CA50 data between the DI and PM tests, showing that premixing 2.3 mg of the fuel in the intake air plenum has the effect of advancing CA50 by nearly 2 CAD on average. Similar trends were observed to a lesser degree for the lower load cases of 11.3 and 10.6 mg of iso-octane; the degree of

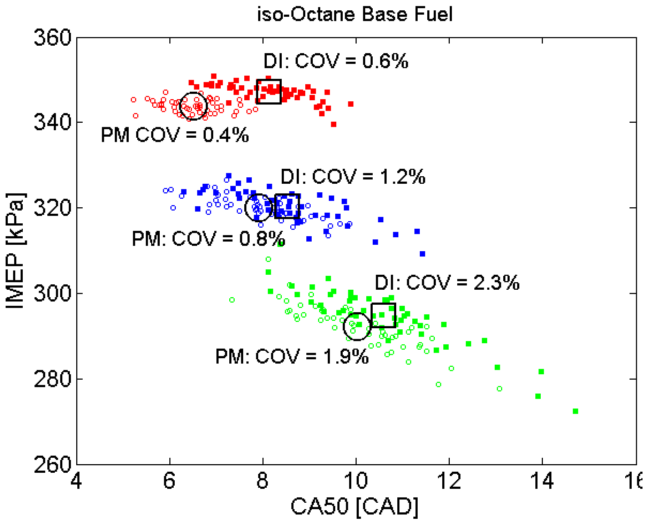

Figure 1. Effect of premixing on iso-octane combustion phasing at three different loads for DI (filled squares) and PM (open circles) tests. Six large symbols represent cycle-averaged values.

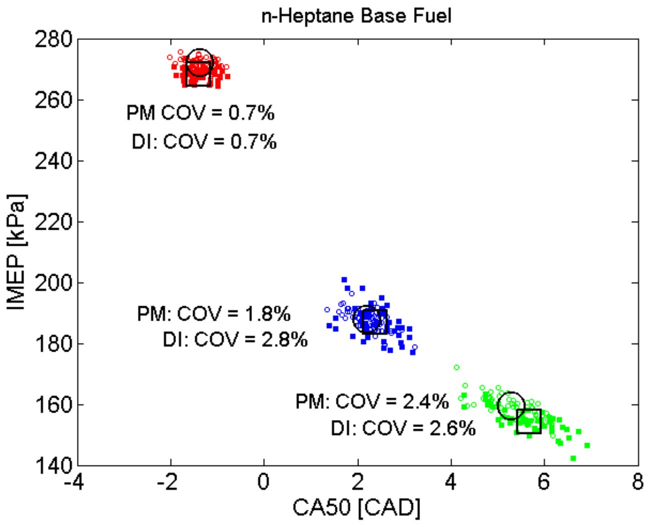

Figure 2. Effect of premixing on n-heptane combustion phasing at three different loads for DI (filled squares) and PM (open circles) tests. Six large symbols represent cycle-averaged values. The prominent spread in loads arises from variations in heating values associated with the different premixed components.

advancement scales by the fraction of total fuel mixed upstream in the plenum.

The advancement of iso-octane combustion with increasing amount of premixing is apparently caused by an elevation in charge temperature. Before arriving in the cylinder, the premixed fuel has already acquired the necessary energy to vaporize and reach the temperature of the surrounding air (480 K). By contrast, when this fuel is instead directly injected in the cylinder at the coolant temperature of 363 K (as in the DI test), there is a relative depression of charge temperature due to lower initial fuel temperature and additional evaporative cooling—combustion is retarded as a result.

The effect of premixing was also examined for three load levels of n-heptane base fuel. The amount of direct-injected n-heptane was maintained at 7.3 mg for each PM test, the results of which are plotted with DI tests in Figure 2. For this two-stage fuel, there is little separation between mean CA50 values for the PM and DI tests—we again look to charge temperature for an explanation.

Because the n-heptane experiments require intake-air and cooling-water temperatures of only 333 K, direct-injected fuel enters the cylinder at about the same temperature as the premixed fuel. Still there are the differences in latent heat that must result in different charge temperatures for the two cases. The CHEMKIN model helps explain why the combustion phasing of n-heptane is only minimally affected by these charge temperature differences.

Simulated pressure traces using CHEMKIN (Figure 3) demonstrate that n-heptane combustion phasing is less sensitive to charge temperature than iso-octane. Although the load and intake temperatures differ between iso-octane and n-heptane, combustion simulations are at conditions similar to the experiments. Increasing the charge temperature by 15 K for iso-octane advances the peak pressure by nearly 10 CAD; whereas an increase of 30 K for n-heptane advances the peak pressure by less than 3 CAD. This relative insensitivity of n-heptane combustion to charge temperature for these experiments is consistent with more general findings of Sjoberg and Dec [22].

These trends explain why we observe little difference in the main combustion phasing of n-heptane when a fraction of the fuel is premixed upstream of the cylinder. Although the amount of evaporative cooling is reduced for the PM case, the relative increase in charge temperature is not enough to cause an observable impact on the main combustion phasing in the experiments.

In addition to observed variations in the main combustion phasing, small variations in the mean IMEP (less than 2%) between PM and DI tests are also apparent, especially for the iso-octane base fuel experiments. Part

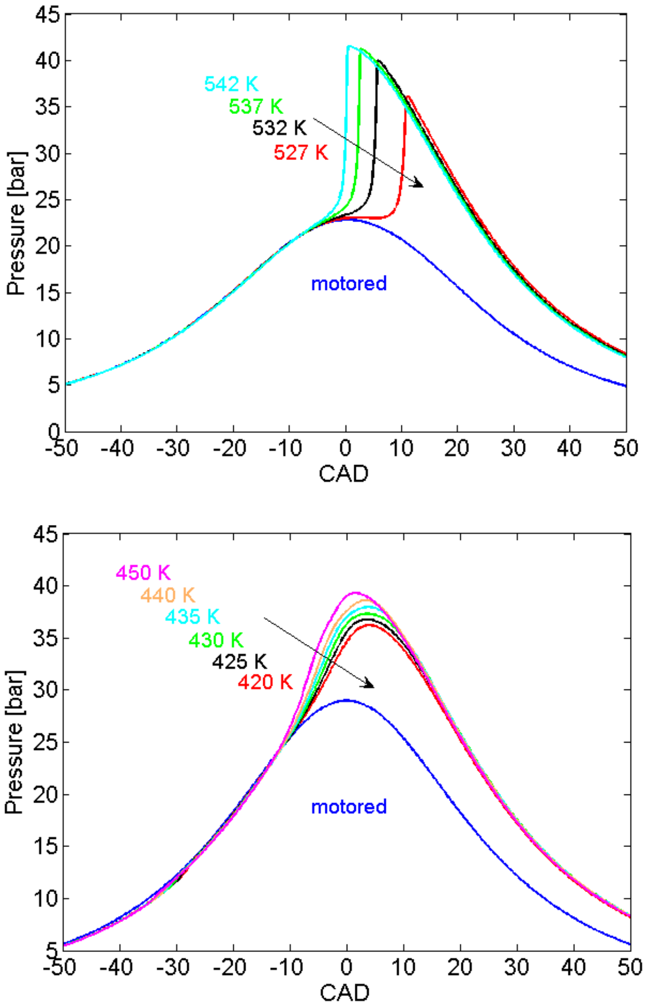

Figure 3. CHEMKIN simulations showing combustion phasing sensitivity to charge temperature for iso-octane (top) and n-heptane (bottom).

of the variation may be attributed to differences in combustion phasing, which impacts both overall heat loss and indicated work. Some of the variation in mean IMEP may also be attributed to small differences in the total amount of fuel delivered. Although repeatable, the performance of the direct injector is sensitive to temperature variations during NVO operation. It is believed that this also leads to generally higher observed COV of IMEP for the DI tests, for which all of the fuel is delivered by the injector.

CHEMICAL EFFECT OF TRACER ON ISO-OCTANE COMBUSTION

Having established the effect of premixing the fuel, the effect of tracer on combustion is now examined by comparing PM and TR tests. In Figure 4, results for substituting an equivalent amount of acetone tracer for iso-octane (along with results for other tracers) are shown in an IMEP vs. CA50 plot. Substituting acetone (TR test) further delays an already late heat release for the PM test by nearly 1.5 CAD. Cycle and average values of IMEP are also observed to decline with phasing retard—consistent with reduced thermal efficiency for heat release occurring later in the expansion stroke. Pressure and heat-release profiles for the three iso-octane-fuel/acetone-tracer tests are shown in Figure 5—the lower and later TR heat-release-rate curve again highlights the reducing and retarding effect of acetone on iso-octane combustion.

CHEMKIN simulations of heat-release profiles for the PM and acetone-TR cases are shown in Figure 6. The rates and duration of heat release deviate from the experimental results largely because a simplistic single-zone combustion model is employed. For this reason, the heat-release rate curves have been normalized (using the peak value of one of the curves). Consistent with the experimental observations, the simulations predict a delay in main heat release for the acetone/TR case on the order of 1 CAD. We conclude that the addition of acetone has a retarding effect on the combustion of iso-octane, as addressed in more detail in the Discussion section.

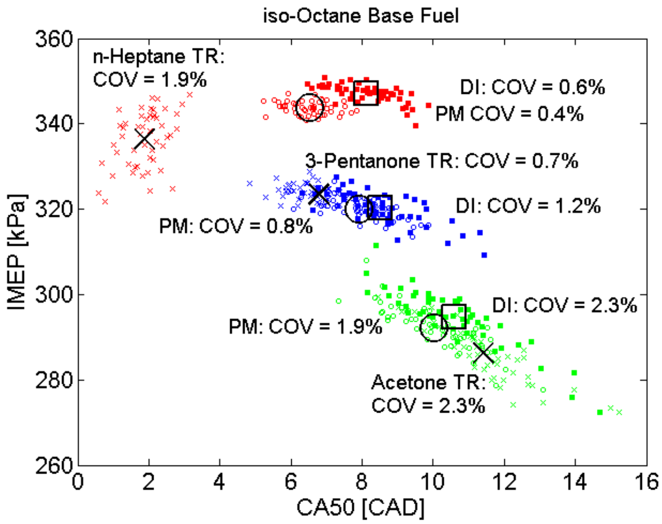

Figure 4. Chemical effect of tracers on iso-octane combustion phasing and IMEP for DI (filled squares), PM (open circles), and TR (X) tests. Nine large symbols represent cycle-averaged values.

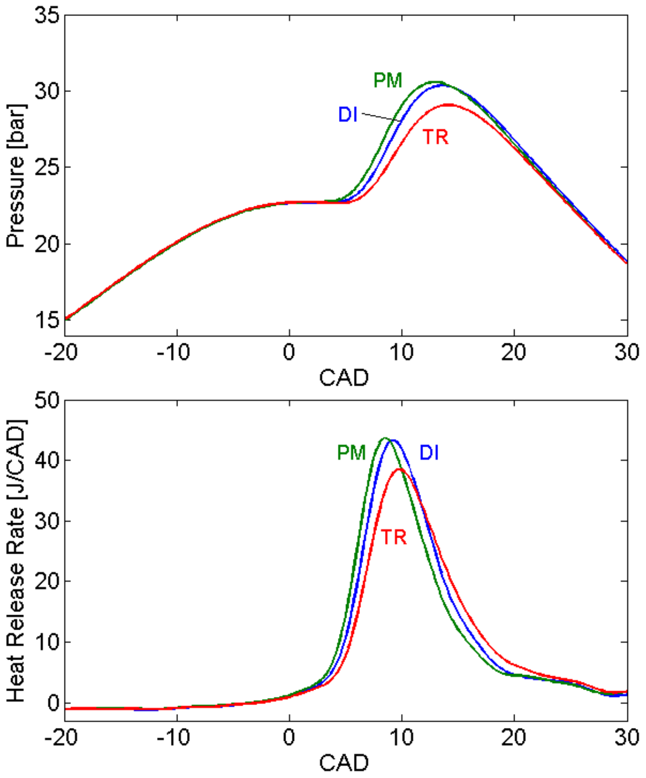

Figure 5. Pressure and heat-release profiles for iso-octane base fuel with acetone seeding.

We now turn to the second tracer, 3-pentanone (iso-octane-fuel/3-pentanone-tracer tests), and find that its effect on combustion is surprisingly the reverse of acetone. Comparing the PM and TR data for 3-pentanone in Figure 4, we see that this tracer moderately increases IMEP while advancing CA50 by more than 1 CAD. In Figure 7, the TR heat-release-rate profile is

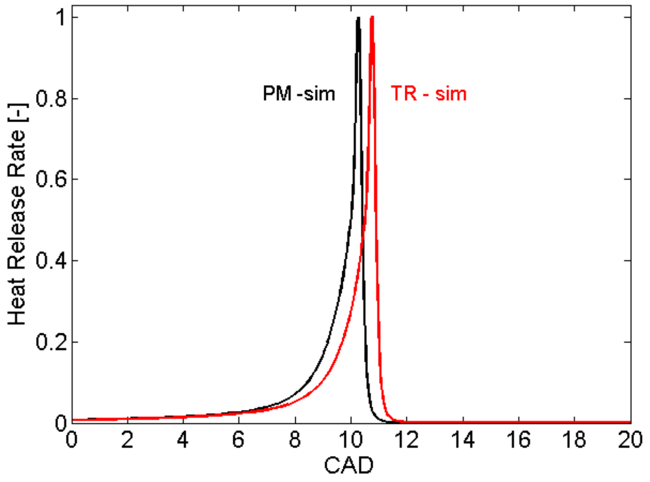

Figure 6. Simulated heat-release profile for iso-octane with acetone seeding.

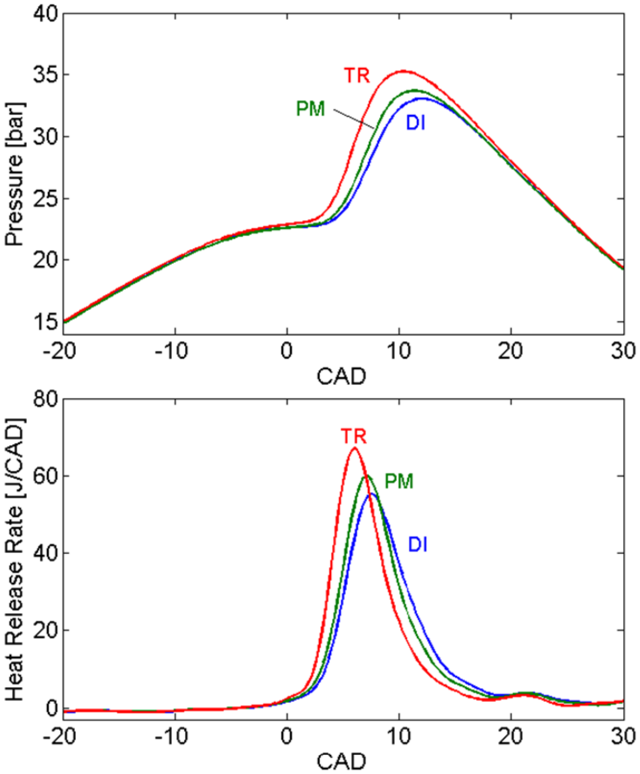

Figure 7. Pressure and heat-release profiles for iso-octane base with 3-pentanone seeding.

taller and earlier than the others, reiterating 3-pentanone's combustion enhancement.

Despite the noted trend reversal when switching tracers, CHEMKIN nonetheless correctly predicts the influence of tracer on heat-release rate and phasing for the 3-pentanone case. The top plot of Figure 8 shows reasonable agreement (considering the 0D model used) of simulated and experimental PM pressure curves. Comparing the simulated PM and TR curves on both plots indicates an earlier (~2 CAD) and more intense heat release when 3-pentanone is substituted for a portion of the iso-octane and premixed in the intake air. This simulated trend is consistent with the experiments, and both indicate that 3-pentanone advances and increases the heat-release rate of iso-octane during HCCI combustion.

Although substitution of 3-pentanone clearly advances the combustion of iso-octane, it does so without a noticeable LTHR (see Figure 7). Examining results for our third tracer (n-heptane in this case of iso-octane base fuel) offers another point of comparison. Results of the iso-octane-fuel/n-heptane-tracer tests are plotted in Figure 9 (and Figure 4) where the TR heat-release-rate curve is significantly advanced (>4 CAD) compared to the PM case. The trend is the same as for 3-pentanone, but the effect is even more pronounced. While it is difficult to compare TR and PM heat-release-rate curves in Figure 9 due to their offset, the TR pressure curve (top plot) appears slightly elevated just prior to the start of main heat release — this is possible evidence of n-heptane LTHR reactions. Of course, the relatively small fraction of n-heptane used as tracer diminishes this expected effect.

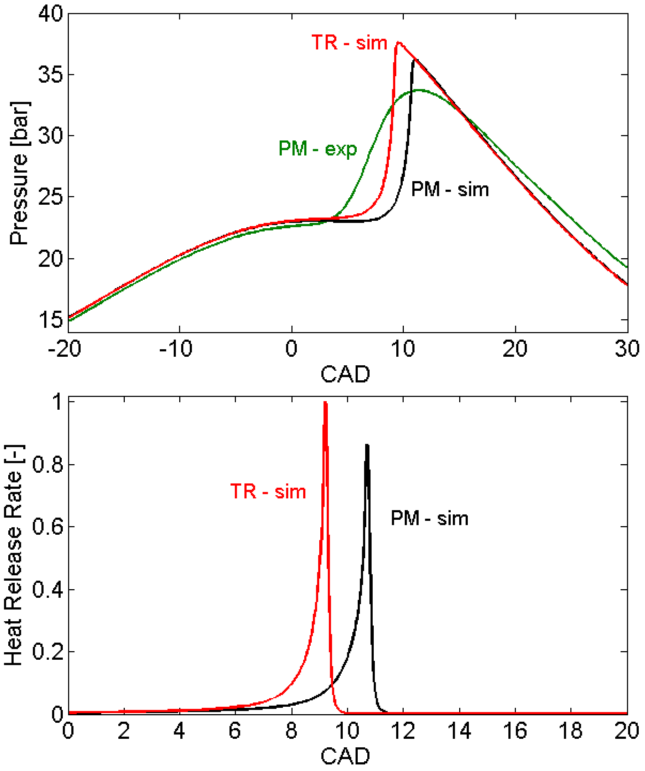

Figure 8. CHEMKIN simulations of pressure (top) and HR profiles (bottom) for iso-octane with 3-pentanone seeding.

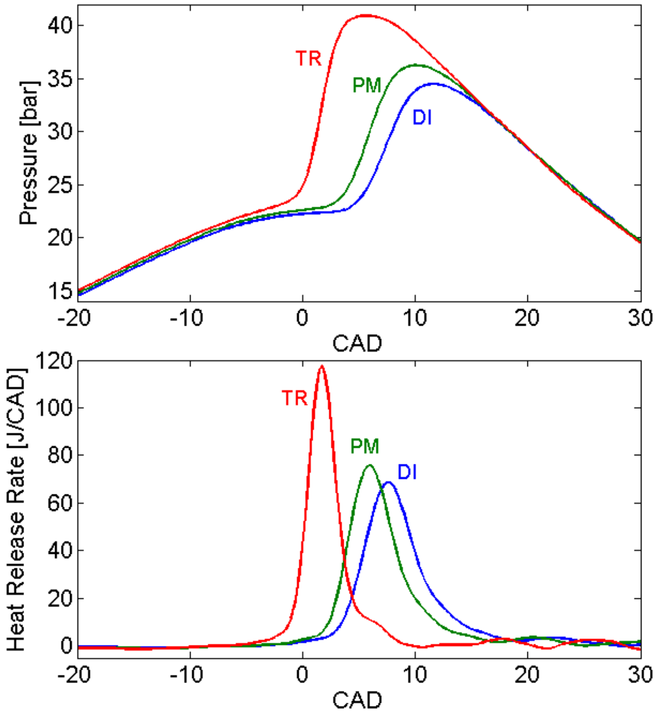

Figure 9. Pressure and heat-release profiles for iso-octane base fuel with n-heptane seeding.

CHEMICAL EFFECT OF TRACER ON N-HEPTANE COMBUSTION

We begin our consideration of the n-heptane-base-fuel experiments by looking at the third tracer in Table 5 (iso-octane). Using iso-octane as tracer in these tests allows us to assess the effect of reducing the fractional amount of two-stage fuel (n-heptane), and serves as a reference case for the other two tracers. In Figure 10, IMEP and phasing of main heat release are plotted for all the n-heptane-base-fuel experiments; the iso-octane tracer results are at the top. While PM and DI cases are nearly identical in IMEP and CA50, the TR case in which iso-octane is substituted for the base fuel shows a nearly 4 CAD retard in phasing. Examining the corresponding heat-release profiles for these tests in Figure 11 shows that the retard of the main heat release is tied to the LTHR of the two-stage fuel, which occurs between -25 and -20 CAD. Replacing premixed n-heptane (PM) with iso-octane (TR) results in a reduction in the rate and amount of the LTHR (likely due to the reduction in the fraction of two-stage ignition fuel) compared to the PM test. A slight retard in peak LTHR is also apparent. Both trends lead to lower temperatures and pressures (at a given CA), and a delayed and slower main burn for the n-heptane/iso-octane mixture.

Prominent in all the heat-release-rate curves in Figure 11 is a late, secondary bump in the main heat release. This feature is likely caused by late conversion of CO to CO_2 as supported by the CHEMKIN simulation of the DI case shown in Figure 12. The main heat release peaks early and is already dropping at TDC when the CO concentration is at a maximum. Soon after, rates of CO consumption and CO_2 production are at their maxima near 5 CAD aTDC, causing an extended main heat release indicated by the secondary bump in both the simulated and experimental profiles. This phenomenon was observed for this early-phased, high-load case because combustion temperatures are high enough to efficiently convert CO to CO_2 [23]. It is not seen in other n-heptane results (to be shown below), likely due to relatively late phasing, lower efficiency, and low CO to CO_2 conversion.

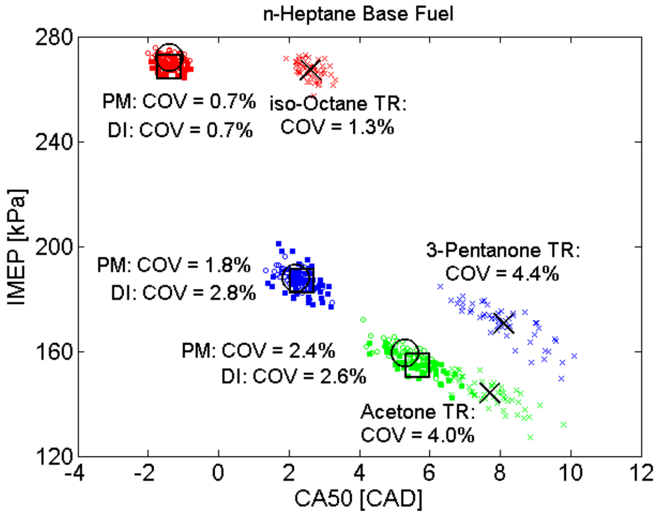

Figure 10. Chemical effect of tracers on n-heptane combustion phasing and IMEP for DI (filled squares), PM (open circles), and TR (X) tests. Nine large symbols represent cycle-averaged values.

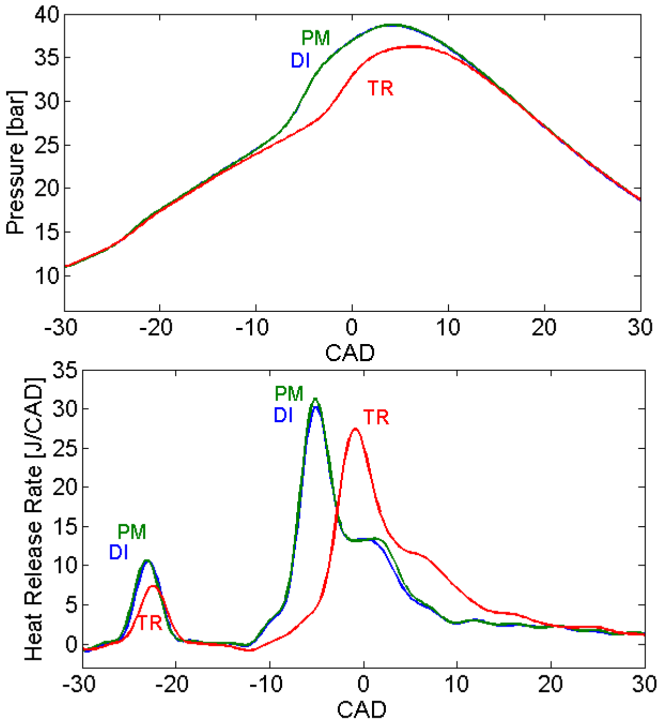

Figure 11. Pressure and heat-release profiles for n-heptane base fuel with iso-octane seeding.

In marked contrast to the advance in phasing caused by adding 3-pentanone tracer to iso-octane discussed in the previous section, substituting the same tracer for n-heptane greatly retards the phasing of the main heat release. The 3P/TR results in Figures 10 and 13 show that CA50 of the main heat release retards by more than

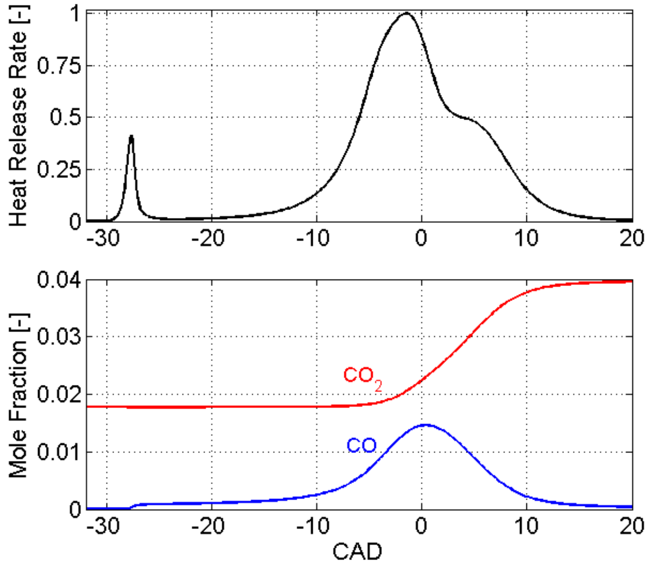

Figure 12. CHEMKIN simulation showing late burnout of CO to CO_2 for n-heptane base fuel.

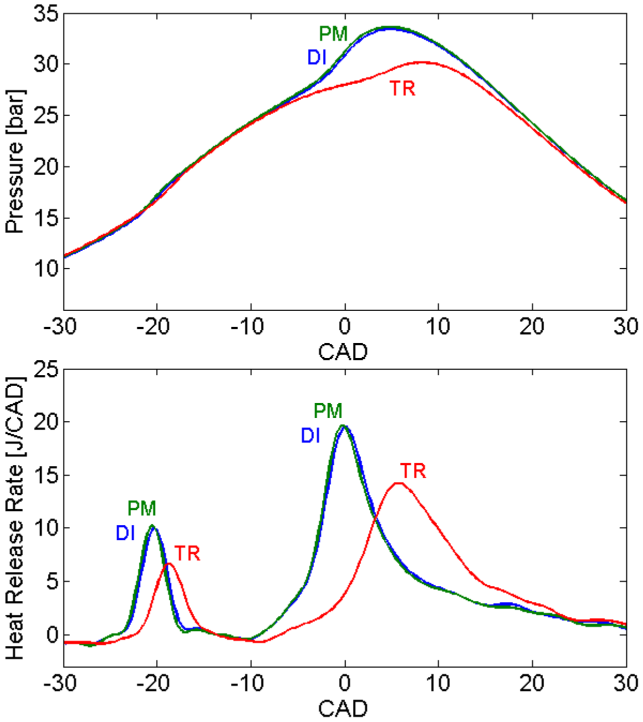

Figure 13. Pressure and heat-release profiles for n-heptane base fuel with 3-pentanone seeding.

6 CAD and IMEP drops by more than 8% from that of the PM test. The relationship between IMEP and phasing can also be seen by examining the scatter of the single-cycle data points in Figure 10. The spread in the data is quantified by a COV of IMEP greater than 4% (more than double that for the related PM test), with later-phased combustion associated with lower IMEP and earlier-phased combustion by higher IMEP. Figure 13 shows a reduced total amount of LTHR for the 3-pentanone mixture, as expected for a reduced fraction of two-stage fuel; but in contrast to the case of iso-octane "tracer" and n-heptane base fuel in Figure 11, initiation and peak of the LTHR are both delayed by nearly 2 CAD.

One possible explanation for this observed delay in LTHR is that the estimated BDC temperature is 4K lower than that of the PM test, due to cooler residual gases. However, an isentropic compression calculation based on measured pressures reveals that temperature at the time of LTHR initiation is actually higher for the 3-pentanone test. For this TR test, the estimated temperature at initiation of LTHR (about 22 CAD bTDC) is 830 K. For the PM test, LTHR begins ~2 CAD earlier, at an estimated temperature of 820 K. The fact that LTHR initiation requires a higher temperature for the 3-pentanone-seeded case suggests that 3-pentanone inhibits low-temperature reactions during n-heptane combustion. This conclusion is supported by our CHEMKIN simulations discussed next.

CHEMKIN simulations in Figure 14 show that decreasing the amount of n-heptane causes a drop in the LTHR with little change in its phasing (curves a → b). When 3-pentanone is added, the LTHR is further reduced and

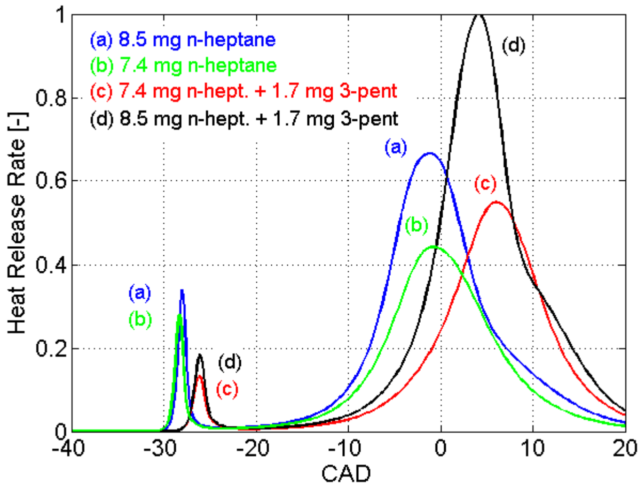

Figure 14. CHEMKIN simulations showing effect of reducing n-heptane and adding 3-pentanone on heat-release profiles.

retards by 3 CAD (curves b → c). The same degree of retard is also observed if 3-pentanone is added without reducing the n-heptane amount (curves c → d). In both the simulations and the experiments, the tracer 3-pentanone clearly inhibits and slows n-heptane combustion, specifically by affecting the low-temperature heat release. The delay in both LTHR and its associated pressure rise leads to a retard in the main heat release, which occurs at lower rates and over a longer duration despite maintaining total HOC (curves a → c).

Combustion trends of n-heptane seeded with the remaining tracer, acetone, are similar to the 3-pentanone tracer case, but vary in degree. We found that for the same intake temperature (333 K), and the same mass of direct-injected n-heptane as the 3P/TR case, acetone seeding led to very late combustion and misfire. This was partially due to the relatively small amount of acetone (and consequently small overall load) needed to achieve target seeding levels in air of 0.15 mol% (Table 5). To be able to continue these tests, we increased intake temperature until stable combustion was achieved at a temperature of 338 K.

The result, seen in Figure 10, is a retard of main heat release (represented by CA50) by ~3 CAD when compared with the corresponding PM case, despite the fact that intake temperature was increased by 5 K. As in the case of seeding with 3-pentanone, the IMEP also drops as combustion efficiency decreases with retarded heat release phasing. Figure 15 presents pressure and heat-release rate profiles for acetone mixed in the intake air at a temperature of 338 K. Consistent with previous cases tested, the magnitude of LTHR falls with the reduction of two-stage fuel (TR @ T_{in} = 338 K curve compared to PM curve), although in this case, LTHR phasing is unchanged despite the higher intake temperature. The effect on main heat release (from -10 to +20 CAD) for this TR case is a modest retardation and reduction in rates compared to the PM case.

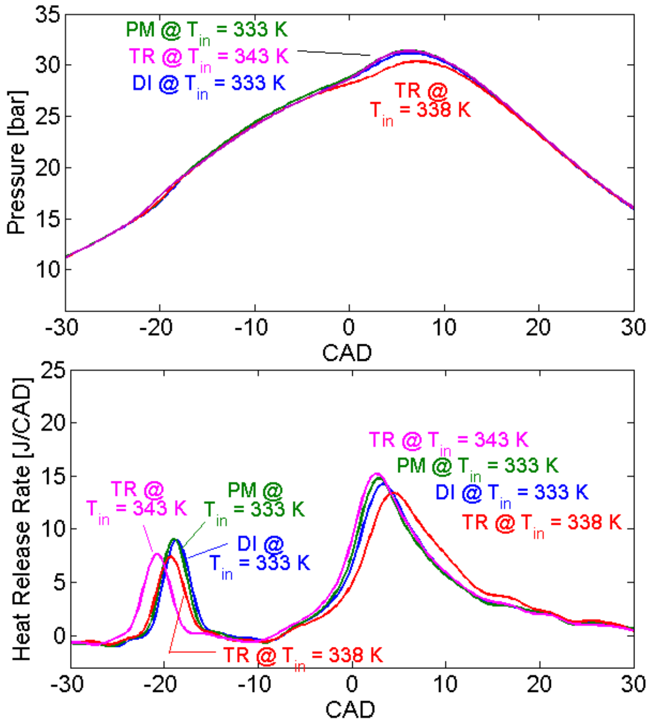

Figure 15. Heat release profiles for n-heptane base fuel with and without acetone seeding over a range of intake air temperatures (T_{in}).

It is interesting to note that increasing intake temperature further to 343 K (TR @ T_{in} = 343 K in Figure 15), advances LTHR sufficiently to recover the phasing and peak rates of the main heat release. We conclude that a modest increase in intake temperature can offset the inhibiting effect of acetone on low-temperature chemistry, allowing us to achieve combustion conditions similar to unseeded operation. CHEMKIN simulations for acetone also support this conclusion.

Discussion

Having presented measurements and simulations of the chemical effect of acetone and 3-pentanone tracers on HCCI combustion for single- and two-stage-ignition fuels, in this section we provide additional support for our observations and investigate potential causes.

In general, substituting tracers for fuel while maintaining total HOC has been shown to affect primarily the phasing of HCCI heat release. Since combustion phasing is an ignition phenomenon, we applied CHEMKIN to estimate ignition times for mixtures resembling those of our experiments in hopes of gaining insight. Figure 16 presents ignition delay times for homogeneous combustible mixtures that are taken to an elevated temperature and pressure at time zero. Plotting limits include time scales and temperatures relevant to our engine experiments. Results agree with experimental shock tube data [24] to within 40% for iso-octane and within 25% for 3-pentanone and acetone.

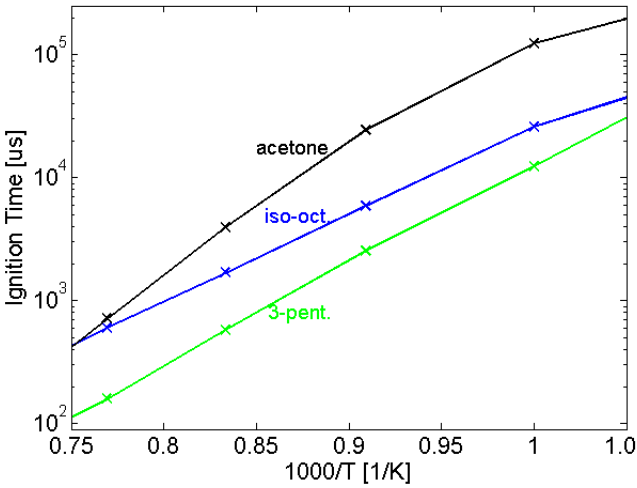

Figure 16. Simulated ignition delay times versus temperature for tracers and iso-octane. Conditions: stoichiometric fuel + oxygen in argon at 12 bar.

The plotted values in Figure 16 indicate that acetone has longer ignition times, and 3-pentanone shorter ignition times, than iso-octane over the temperature range and time scales of interest in this study. For the iso-octane/tracer experiments conducted in this study, ignition occurred approximately 10 CAD after TDC in all cases. Estimated near-TDC charge temperatures are about 1200K (1000/T = 0.83), which corresponds to an ignition time for iso-octane on the order of a few milliseconds or 10-20 CAD at 1200 RPM. This is consistent with experimentally observed values if we compute ignition delays from 10 CAD bTDC (when temperatures reach the 1200 K level). Based on ignition times in Figure 16 for tracers at the same temperature, one would expect acetone, which has a slower ignition time, to retard iso-octane combustion, and 3-pentanone, which has a faster ignition time, to advance iso-octane combustion. These trends are consistent with our experimental results.

The process of ignition of n-heptane differs profoundly from the other three molecules studied because of its low-temperature chemistry. Because gas temperatures in the above simulations are instantly elevated at time zero rather than being ramped through the low-temperature-reaction regime, such computations are not well suited for comparisons of tracer and n-heptane ignition delay data. For further insights into tracer-n-heptane interactions, we return now to detailed reaction data from our CHEMKIN engine simulations.

Figure 17 shows the time variation of radical species concentrations during the low-temperature heat release of n-heptane for two simulated conditions. The solid curves represent n-heptane combustion and the dashed curves represent n-heptane plus 3-pentanone. Conditions correspond to those of the simulated pressure and heat-release profiles shown in Figure 13. In the plot, an abrupt decrease in radical species concentrations occurs near the peak of LTHR. Prior to this point, we see that 3-pentanone seeding is associated with much smaller production rates of important radical species—at a given

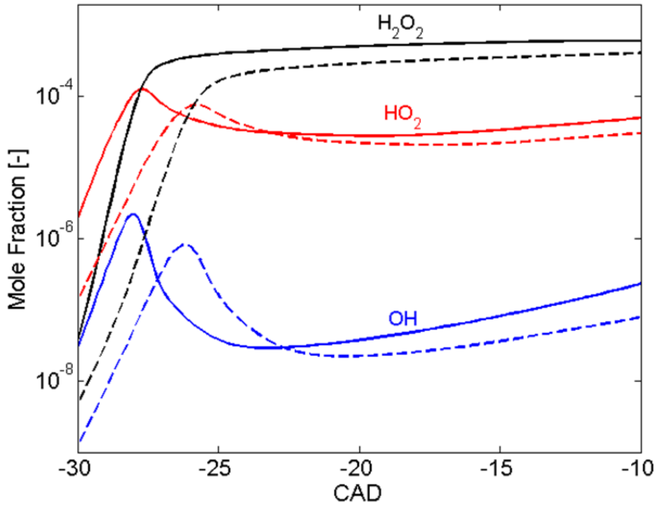

Figure 17. Simulated radical species concentrations prior to and during LTHR for n-heptane combustion with 3-pentanone seeding (dashed lines) and without (solid lines).

CAD, concentrations of HO_2, OH, and H_2O_2 are all more than an order of magnitude lower (dashed curves) than in the pure n-heptane case (solid curves). As a result, the amount and peak of LTHR are reduced and delayed, as shown previously in Figures 13 and 14.

Further confirmation of the effect of 3-pentanone on LTHR is shown in Figure 18. The simulated progress of reaction for 3-pentanone and n-heptane decomposition is plotted for mixtures with and without 3-pentanone. Comparison of the curves shows that the 3-pentanone decomposition reaction takes off well before that of n-heptane. The 3-pentanone decomposition reactions reduce the radical populations involved in LTHR (Figure 17), and consequently delay the decomposition of n-heptane as witnessed by the dashed n-heptane curve shifting to the right in Figure 18.

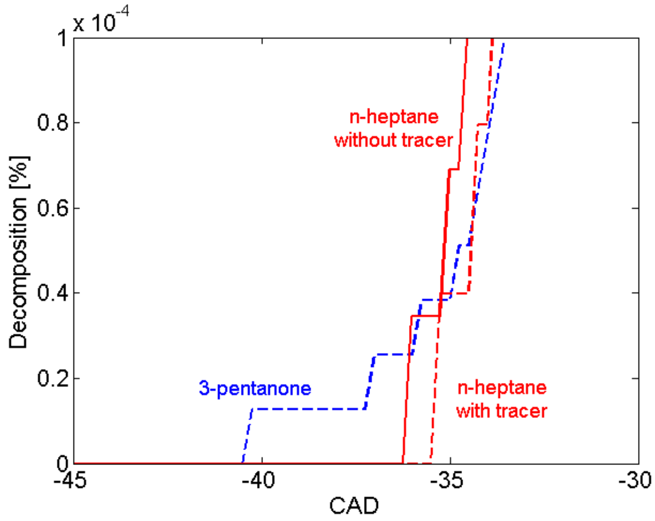

Figure 18. Progress of 3-pentanone and n-heptane decomposition prior to LTHR for n-heptane combustion with 3-pentanone seeding (dashed lines) and without (solid line).

CONCLUSIONS

The chemical and thermal effects of seeding intake air with fluorescent tracers have been characterized in our DI HCCI engine. In contrast to previous studies of seeding effects on SI engine performance and flame propagation, this work has shown that tracers have a measureable impact on combustion phasing for HCCI operation. The chemical effect of seeding is more pronounced for n-heptane base fuel, largely because of tracer interactions with low-temperature reactions: Adding 3-pentanone or acetone to n-heptane inhibits and retards LTHR reactions, potentially leading to a delay of main heat release by more than 6 CAD. These chemical effects are in addition to changes in combustion associated with reducing the fraction of two-stage fuel as tracer is substituted for n-heptane. Thermal effects of tracer seeding are more pronounced for iso-octane combustion because of its greater sensitivity to variations in charge temperature. Substituting tracer for DI fuel and premixing it in the intake plenum can significantly reduce the DI charge-cooling effect while also modifying charge temperature through differences in supplied sensible energy.

Overall, the impact of tracer seeding on combustion behavior is modest enough to overcome by choosing an appropriate offset such as increasing or decreasing intake temperature. By applying modest offsets, understanding the general impact of tracer seeding on combustion, and using this knowledge to properly interpret measurements, PLIF diagnostics using air seeded with fluorescent tracers may be reliably applied to HCCI combustion.

ACKNOWLEDGMENTS

Research at Sandia was supported by the U.S. Department of Energy, Office of Vehicle Technologies. Sandia is a multiprogram laboratory operated by Sandia Corporation, a Lockheed Martin Company, for the United States Department of Energy's National Nuclear Security Administration under contract DE-AC04-94AL85000. Research at Stanford University was sponsored by Nissan Motor Co., Ltd.

REFERENCES

1. Schulz, C. and Sick, V., "Tracer-LIF Diagnostics: Quantitative Measurement of Fuel Concentration, Temperature, and Fuel/Air Ratio in Practical Combustion Systems," *Prog. Energy Combust. Sci.* **31**:75-121, 2005.
2. Zhao, H. and Ladommatos, N., "Optical Diagnostics for In-Cylinder Mixture Formation Measurements in IC Engines," *Prog. Energy Combust. Sci.* **24**:297-336, 1998.
3. Fujikawa, T., Fukui, K., Hattori, Y., and Akihama, K., “2-D Temperature Measurements of Unburned Gas Mixture in an Engine by Two-Line Excitation LIF Technique,” SAE Paper 2006-01-3336, 2006.
4. Nagamine, M., Kakuho, A., Amenomori, Y., Urushihara, T., and Itoh, T., “In-Cylinder Mixture Temperature Distribution Measurement for HCCI Combustion,” SAE Paper 2006-05-0198, 2006.
5. Rothamer, D. A., Snyder, J., Hanson, R. K., and Steeper, R. R., “Two-Wavelength PLIF Diagnostic for Temperature and Composition,” SAE Paper 2008-01-1067.
6. Rothamer, D. A., Snyder, J. A., Hanson, R. K., Steeper, R. R., and Fitzgerald, R. P., "Simultaneous Imaging of Exhaust Gas Residuals and Temperature During HCCI Combustion," *Proceedings of the Combustion Institute*, 2008.
7. Deschamps, B. and Baritaud, T., “Visualization of Gasoline and Exhaust Gases Distribution in a 4-Valve SI Engine; Effects of Stratification on Combustion and Pollutants,” SAE Paper 961928, 1996.
8. Neij, H., Johansson, B., and Alden, M., "Development and Demonstration of 2D-LIF for Studies of Mixture Preparation in SI Engines," *Combustion and Flame* **99**:449-457, 1994.
9. Zhang, R., Wermuth, N., and Sick, V., “Impact of Fluorescence Tracers on Combustion Performance in Optical Engine Experiments,” SAE Paper 2004-01-2975, 2004.
10. Ghandhi, J. B. and Felton, P. G., "On the Fluorescence Behavior of Ketones at High Temperature," *Experiments in Fluids* **21**:143-144, 1996.
11. Grossmann, F., Monkhouse, P. B., Ridder, M., Sick, V., and Wolfrum, J., "Temperature and Pressure Dependences of the Laser-Induced Fluorescence of Gas-phase Acetone and 3-Pentanone," *Applied Physics B* **62**:249-253, 1996.
12. Koch, J. D. and Hanson, R. K., "Temperature and Excitation Wavelength Dependencies of 3-Pentanone Absorption and Fluorescence for PLIF Applications," *Applied Physics B* **76**:319-324, 2003.
13. Ossler, F. and Alden, M., "Measurements of Picosecond Laser Induced Fluorescence from Gas Phase 3-Pentanone and Acetone: Implications to Combustion Diagnostics," *Applied Physics B* **64**:493-502, 1997.
14. De Zilwa, S. and Steeper, R. R., “Acquisition of Corresponding Fuel Distribution and Emissions Measurements in HCCI Engines,” SAE Paper 2005-01-3748, 2005.
15. Heywood, J. B., “Internal Combustion Engine Fundamentals”, McGraw-Hill, 1988.
16. Reaction Design, CHEMKIN 4.1, http://www.reactiondesign.com/products/open/chemkin.html, 2007.
17. Lawrence Livermore National Laboratories, Combustion Chemistry, http://www-cmls.llnl.gov/?url=science_and_technology-chemistry-combustion, 2008.
18. Curran, H. J., Gaffuri, P., Pitz, W. J., and Westbrook, C. K., "A Comprehensive Modeling Study of iso-Octane Oxidation," *Combustion and Flame* **129**:253-280, 2002.
19. Curran, H. J., Gaffuri, P., Pitz, W. J. and Westbrook, C. K., "A Comprehensive Modeling Study of n-Heptane Oxidation" *Combustion and Flame* **114**:149-177, 1998.
20. Curran, H. J., Pitz, W. J., Westbrook, C. K., Callahan, C. V., and Dryer, F. L., “Oxidation of Automotive Primary Reference Fuels at Elevated Pressures,” *Proceedings of the Combustion Institute* **27**:379-387, 1998.
21. Dec, J. E. and Sjoberg, M., “Isolating the Effects of Fuel Chemistry on Combustion Phasing in an HCCI Engine and the Potential of Fuel Stratification for Ignition Control,” SAE Paper 2004-01-0557, 2004.
22. Sjoberg, M. and Dec, J. E., "Comparing Late-Cycle Autoignition Stability for Single- and Two-Stage Ignition Fuels in HCCI Engines," Proceedings of the Combustion Institute **31**:2895-2902, 2007.
23. Sjoberg, M. and Dec, J. E., "An Investigation into Lowest Acceptable Combustion Temperatures for Hydrocarbon Fuels in HCCI Engines," *Proceedings of the Combustion Institute* **30**:2719-2726, 2005.
24. Stanford University Mechanical Engineering Department, Fundamental Kinetics Database Utilizing Shock Tube Measurements, http://hanson.stanford.edu/research/kinetics/kinetics.htm, 2008.